Journal of Nuclear Materials 381 (2008) 15–24

Contents lists available at ScienceDirect

Journal of Nuclear Materials

journal homepage: www.elsevier.com/locate/jnucmat

Practical aspects for characterizing air oxidation of graphite

Cristian I. Contescu [a,*], Samina Azad [b], Doug Miller [b], Michael J. Lance [a], Frederick S. Baker [a], Timothy D. Burchell [a]

[a] Oak Ridge National Laboratory, UT-Battelle Inc., P.O. Box 2008, Oak Ridge, TN 37831, United States
[b] GrafTech International, Parma, OH 44130, United States

A B S T R A C T

The efforts for designing a meaningful and acceptable standard test method for characterization of kinetic parameters of air oxidation of graphite helped identify several practical issues that must be considered for the development of such a test. Using standard size (and shape) specimens, large enough in size to accommodate the inherent local microstructure differences between graphite samples, resulted in non-uniform oxidation profiles and preferential binder oxidation; this was not expected based on the linearity of Arrhenius plots and the (large) values of activation energy. It was found that the transition between the regimes 1 and 2 of graphite oxidation occurs gradually, depending both on the oxidation temperature and rate of oxygen supply. Nevertheless, measuring oxidation rates obtained on standard size samples provides a basis for a meaningful comparison among materials, which may serve as much needed information for predictive models.

1. Introduction

Studies focused on the oxidation of graphite are of considerable interest because of the extensive use of graphite materials in nuclear reactors. High temperature gas-cooled reactors are expected to become the next generation of nuclear reactors. One of the most critical safety factors that must be considered during operation of this type of reactor is the event of an air-ingress incident, during which the graphite in the moderator and reflector are exposed to oxygen at high temperature [1].

In order to define a meaningful, generally accepted standard test method for characterizing air oxidation of graphite [2], one must first identify the test conditions for which the perturbing influence of experimental factors (sample geometry and size, air flow distribution, local temperature gradients) is minimal. Ideally, under such test conditions, only the intrinsic material properties (crystallite size and morphology, impurity content, etc) would be measured; this would permit a clear differentiation between materials for selection purposes, and would improve quality control during fabrication. However, this task is not straightforward, as shown previously by many other researchers [3–7] and demonstrated again by new reports on the effects of sample size [8] or shape [9] on rates of graphite oxidation.

Graphite oxidation in air is controlled by chemical kinetics at low temperature, but becomes diffusion-limited at high temperatures [10,11]. In the low temperature limit (regime 1) the oxidation rate depends on gas phase oxygen concentration and on intrinsic material reactivity, which in turn depends on the material's microstructure. As the temperature increases, oxidation rates become more sensitive to surface oxygen concentration (and thus to air flow conditions), and the mechanism shifts to in-pore diffusion control (regime 2). At even higher temperatures oxidation is strictly limited to the surface layer (regime 3) and is controlled by the mass transfer of gas species (O_2, CO, CO_2) through the boundary layer at the solid/gas interface. In this range, oxidation rates are not material-dependent and kinetic measurements were not deemed necessary [12].

The increase in porosity throughout the volume of graphite during oxidation in regimes 1 (and to a lesser extent in regime 2) has a high impact on mechanical properties of graphite. Therefore an in-depth examination of the oxidation kinetics of graphite materials in regimes 1 and 2 is essential. The relationship between intrinsic material properties (such as the size, shape and crystallinity of component graphite grains, distribution of internal porosity, impurity content in the binder, etc) and the kinetic parameters, including temperature limits for oxidation in regimes 1 and 2, are still not well understood. Using graphite samples in powder form for measurements of oxidation rate by thermogravimetric analysis (TGA) may, in principle, provide basic kinetic parameters. However, it was reported that, even for powdered samples, oxidation rates free of diffusion effects could only be measured for sample weights of 5–10 mg and air flow rates of 100 mL/min [4]. The effects of diffusion and material morphology during oxidation become increasingly important for machined samples, beginning with sizes of several millimeters and weights of several milligrams. Such

* Corresponding author.
E-mail address: ccontescu@ornl.gov (C.I. Contescu).

0022-3115/$ - see front matter © 2008 Published by Elsevier B.V.
doi:10.1016/j.jnucmat.2008.07.020

samples can be accommodated by most commercial TGA instruments, but it is not warranted to predict oxidation behavior of large monolithic graphite blocks based on simple extrapolation of results obtained for powdered, or small-size machined specimens.

Nuclear graphite is a non-homogeneous composite material consisting of filler particles and a binder. According to current standard specifications [13], the filler particle size in the mix formulation for nuclear graphite may be as large as 1.68 mm. According to another classification [14], grain sizes in medium grained graphite cover a broad range, generally between 100 μm and 4 mm; the grain sizes of ultrafine and microfine varieties are smaller than 10 μm and 2 μm, respectively. This broad range of grain sizes, combined with the presence of micropores, voids, agglomerates, inclusions, and atypical grains, contributes to large variations in the local microstructure. This not only affects graphite mechanical properties, but is also reflected in gas diffusion properties. For model-developing purposes, it was suggested that the characteristic dimension of a two-phase porous medium representative of the structure of graphite should be in the range of several centimeters [15]. Accordingly, the practice of sampling graphite specimens for property characterization recommends using large enough specimens, for which material non-homogeneities are averaged (e.g. 200 mm × 20 mm × 15 mm for fracture toughness [16], and 90 mm × 30 mm × 30 mm for Weibull parameters [17]).

This paper reiterates several of the practical issues that became apparent during the development of an ASTM test for characterization of air oxidation of graphite [2]. The test is intended for standardization of oxidation rate measurements and extraction of oxidation rate parameters that can be used as a basis for predictive models. The standardized test may also be used for quality control purposes and will provide a metric for qualification of various types of nuclear graphite. In the form proposed, the test recommends using specimens of standard size and shape, large enough to be representative of the microstructure of the material. By measuring the rate of weight loss upon oxidation in a stream of dry air at several temperatures, the test provides two tiers of information. On the one hand, measurement of oxidation rates at custom-selected temperatures is standardized with respect to sample size, shape, and air flow conditions. On the other hand, the oxidation rates measured at several temperatures can be used to assist in the differentiation of various grades of graphite for estimation of the effective activation energy. This information can be used in turn as a differentiator of various grades of graphite and may provide input information for predictive models of graphite oxidation available today [18–20].

2. Background

The proposed ASTM test applies correctly to air oxidation under kinetic control (regime 1), where the oxygen supply is not limited by diffusion, and the only reaction is the reaction with O_2 (i.e. the reaction with CO_2, which becomes increasingly important as the temperature increases, is neglected). It is assumed that in the kinetic regime the rate of the chemical reaction between carbon and oxygen is given by the equation:

$$r = -\frac{\Delta m}{\Delta t} = kP^n m \tag{1}$$

where m is the weight of carbon and P is the partial pressure of oxygen, for which a reaction order $n < 1$ was often observed [21]. It is also assumed that the kinetic constant k obeys the Arrhenius relationship with constant activation energy, E_a:

$$k = k_0 \exp(-E_a/RT) \tag{2}$$

There are several ways to normalize oxidation rates. In regime 1, where oxidation is assumed to occur uniformly throughout the bulk, it makes sense to normalize the rate by the mass of the sample, corrected for the actual weight loss. In regimes 2 and 3 oxidation rates become sensitive to the surface-to-volume ratio, and therefore the oxidation rates should be normalized to the exposed surface area. However, if samples of uniform size and shape are used, normalizing by the exposed (geometric) surface area would consider with equal weight both the uniform oxidation through the bulk in regime 1 and those instances (at high temperatures) where diffusion control (regime 2) becomes increasingly important. It should be stressed that normalization by geometric area cannot be used to compare oxidation rates of samples of varying size or shape, even when they are from the same material. The reason is the dependence of the area-normalized oxidation rate, r_a, on the surface-to-volume ratio of specimens, see Eq. (3). This is one of the reasons of large disparities between oxidation rates measured with different sample sizes or different equipment setups, even though the activation energy, E_a, was correctly calculated

$$\begin{aligned}\log_{10}(r_a) &= \log_{10}\left(\frac{1}{A_0}\frac{\Delta m}{\Delta t}\right) \\ &= \left[\log_{10}(k_0) + \log_{10}(P^n) + \log_{10}(\rho_0 \frac{V_0}{A_0})\right] \\ &\quad - \left(\frac{E_a}{2.303R}\right)\frac{1}{T}\end{aligned} \tag{3}$$

If a comparison between oxidation rates measured on samples of different sizes (or on different instruments) is desired, then reaction rates normalized by the weight of the sample, r_m, should be used:

$$\begin{aligned}\log_{10}(r_m) &= \log_{10}\left(\frac{1}{m_t}\frac{\Delta m}{\Delta t}\right) \\ &= [\log_{10}(k_0) + \log_{10}(P^n)] - \left(\frac{E_a}{2.303R}\right)\frac{1}{T}\end{aligned} \tag{4}$$

where m_t, the weight of the sample at time t, rather than m_0, the initial weight, is more appropriate. Even so, this form of kinetic equation (based on regime 1) is not robust enough to accommodate all factors that may vary during the course of oxidation at large weight loss levels, including the 'induced surface heterogeneity and the continuously developing porosity in the material [21]. For practical reasons, and in view of the increased interest in high temperature applications of graphite (regimes 2 or 3), surface-normalized rates were used by more researchers [1,3,12,22–25] than mass-normalized [26–28] or volume-normalized [9,18] rates.

3. Experimental

A home-made experimental setup was used, consisting of a three-zone vertical tube furnace (90 cm long) and an analytical balance with weigh-below port feature. An inconel tube (7.30 cm outer diameter, 6.27 cm inner diameter, 150 cm long) placed inside the furnace extends on both ends. The balance (resolution 0.001 g) is placed on top of the vertical furnace, and is thermally shielded such that it operates at constant (room) temperature. The graphite specimens (cylinders, 2.54 cm diameter and 2.54 cm in height, about 22 g weight) are placed in a Pt wire basket hanging on a thin Pt wire from the weigh-below port of the balance. Care was taken that the graphite specimens were placed in the center of the constant temperature zone of the furnace (about 30 cm long). The sample temperature is measured by a K-type thermocouple placed inside the furnace, not touching it, but not more than 5 mm from the graphite sample. Inert gas (dry, oxygen-free nitrogen) or dry air is introduced from the bottom, passing through a 5 cm layer

of silica gel beads for additional drying and mixing. The test samples are preheated and weight stabilized (60 min) in a flow of dry nitrogen, after which the flow through the vertical tube is switched to dry air (usually 10 L/min). The weight variations are recorded while maintaining the samples in the air flow at constant temperature.

A commercial TGA system (Q600 SDT from TA Instruments) was also used for several tests, and the results obtained using both instruments were compared. The samples used in the TGA system were much smaller in size (cylindrical, 6 mm diameter, 6 mm height) and weighed about 300 mg. The maximum air flow rate achievable in the TGA system is 1 L/min.

Several graphite materials were analyzed. They included a high purity grade from GrafTech International (grade PGX purified, density 1.77 g/cm^3); a highly densified nuclear grade graphite (NBG 10, density 1.81 g/cm^3) and a fine grained graphite (R4-650, density 1.84 g/cm^3), both from SGL; a coarse grained electrode-grade graphite (AG 13-01, density 1.64 g/cm^3) with low ash content (~0.05%) from former UCAR Carbon Company (now GrafTech International); a fine-grained graphite (2020, density 1.64 g/cm^3) with about 0.13% ash content from Carbone-Lorraine North America; and an in-house material press-formed and carbonized (1800 °C) from a mixture of natural graphite and phenolic resin that replicates the composition of matrix fuel compacts for high temperature gas-cooled reactors (density 1.33 g/cm^3).

4. Results and discussion

4.1. Effect of air flow rate

The rate of air supply to the sample was identified as an important factor that caused differences between test results. Increasing the rate of air supply increased the oxidation rates, at constant temperature. This effect was more pronounced at high temperatures, and was larger for the small samples (0.3 g) used in the TGA system than for the large samples (22 g) used in the vertical furnace, as illustrated in Fig. 1. This finding was not surprising, given that the surface-to-volume ratio was much larger for the 6 mm samples used in TGA than for the 25.4 mm samples used in the vertical furnace. Sensitivity to the surface-to-volume ratio indicates that the oxidation was (partially) diffusion-controlled (regime 2) [10], at least at the highest temperature studied (750 °C). The Arrhenius plots were however linear and the activation energy did not show variations larger than 5% between the vertical furnace and the TGA setup (between 600 and 750 °C).

A quick reference to previous literature data is useful at this time. Oxidation rates for the graphite IG 110 were measured by many authors and in various experimental conditions. If one compares the results of various studies, based on published Arrhenius plots (i.e. $\log_{10}(r_m)$ vs. $1/T$) for samples of comparable diameter (D) and height (H) it soon becomes evident that the transition between regimes 1 and 2 moves to higher temperature as the air flow rate increases. For example, at a flow rate of only 0.020 L/min, Xiaovei et al. [29] found that the change of slope of the Arrhenius plot occurred at 600 °C for cylindrical samples with $D = H = 1$ cm (Fig. 5 of Ref. [29]). At a higher flow rate (0.5 L/min for samples with $D = 0.8$ cm and $H = 1.9$ cm) Fuller and Okoh [3] obtained an Arrhenius plot that was linear up to 750 °C (Fig. 4 of Ref. [3]). At a much higher flow rate (40 L/min for samples with $D = 2.1$ cm and $H = 3$ cm) Kim et al. [18] found that the bending of Arrhenius plot occurred at 900 °C (Figs. 8 and 11 of Ref. [18]). From these results it is apparent that the air flow rate, rather than the sample size, is the main factor that affects the transition temperature to the in-pore diffusion regime. Furthermore, the same data were used to calculate that the ratio between the rate of oxygen supply (moles/min) and that of carbon oxidation (moles/min) at the highest temperature where the Arrhenius plot is still linear; the calculated ratios were 9.8 [29], 7.6 [3], and 11.9 [18]. Based on these literature results (although their number is limited) it appears that, at least for samples of 1–2 cm diameter, the oxidation is in the kinetic control (regime 1) as long as the oxygen supply rate is roughly at least 10 times higher than the rate of carbon oxidation. If the oxygen flow rate is less than about 10 times of what would be needed to sustain the rate of carbon oxidation at the highest temperature, the mechanism moves into the in-pore diffusion control (regime 2).

This conclusion is also supported by data of the present study. Fig. 2 compares oxidation rates of standard size samples ($D = H = 25.4$ mm) in the vertical furnace at a constant air flow rate of 10 L/min. For three nuclear grade graphite materials the plots are linear between 600 and 750 °C. As the oxidation accelerates with the increase in temperature, the ratio of oxygen supply rate to carbon loss rate declines, but is always higher than 10, even at the highest temperature. In contrast, a more reactive material (matrix compacts, treated to only 1800 °C and not fully graphitized) shows higher oxidation rates. For this sample the Arrhenius plot bends at a lower temperature (650 °C), where the oxygen supply rate (corresponding to 10 L/min air flow) drops below 10, when

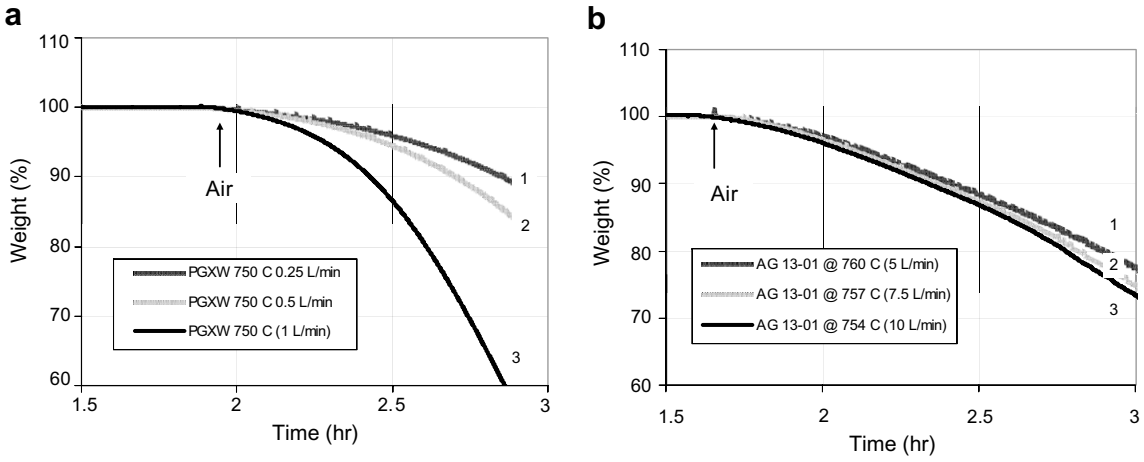

Fig. 1. Effect of air rate supply on oxidation rates measured in (a) a commercial TGA system and (b) in the vertical furnace. The oxidation temperature was 750 °C in both cases. The air flow rate in the TGA system (a) was (1) 0.25 L/min, (2) 0.5 L/min, and (3) 1 L/min. In the vertical furnace (b) the air flow rate was (1) 5 L/min, (2) 7.5 L/min, and (3) 10 L/min. Samples sizes were 0.3 g in the TGA system and 22.5 g in the vertical furnace.

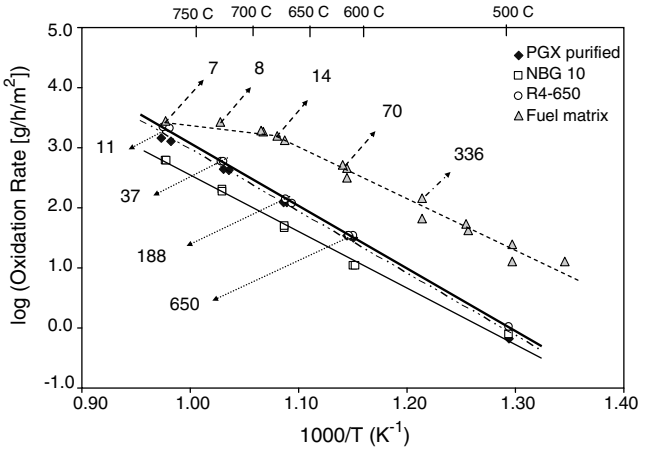

Fig. 2. Effect of air supply rate on linearity of Arrhenius plots. Most oxidation rates were measured in the vertical furnace at constant air flow rate (10 L/min). For three graphitic materials (PGX purified, NBG 10, and R4-650) the measurement at 500 °C was made according to ASTM C-1179 in a muffle furnace with natural convection. For all three graphites the plots are linear up to 750 °C. For the fourth material (fuel matrix partially graphitized) the linearity of the plot breaks at 650 °C. The ratio of oxygen supply rate (moles/min) to carbon loss rate (moles/min) at several temperatures is shown with arrows for the most reactive two materials. Data suggest that Arrhenius plots are linear as long as this ratio is larger than ~10.

compared to the rate of carbon oxidation. The ratio of the two rates is shown with arrows for several data points of the most reactive samples in Fig. 2. The lowering of apparent activation energy for this sample (Fig. 2) signals that the oxidation mechanism has shifted from kinetic control (regime 1) to in-pore diffusion control (regime 2).

4.2. Oxidation depth and density profile of oxidized sample

It is largely assumed that the linearity of Arrhenius plots indicates that oxidation has a unique mechanism [30]; for graphite materials, oxidation in the range of temperatures where the Arrhenius plot is linear is assumed to occur in the kinetic regime 1 (uniformly throughout the volume). In order to verify that assumption, the radial density of several graphite samples (small grained R4-650 material) was measured after oxidation at four temperatures between 600 and 750 °C. In this range the Arrhenius plots were linear (as shown in Fig. 2) and the activation energy (202 kJ/mol; calculated between 5 and 10% weight loss) was in the range expected for graphite oxidation occurring in the chemically controlled regime.

All samples used in this study were cylindrical ($D = H =$ 25.4 mm). The density profile was measured by machining a thin layer (1 mm) from the outer surface of the oxidized samples, and accurately weighing the residual core after each machining step. The density of the layer removed was calculated by comparing with the previous measurements. This operation was repeated until the density of the remaining core approached the density of the unoxidized sample (1.83 g/cm^3). Fig. 3 shows the density profiles at three oxidation temperatures and for two different weight loss levels. Although the density profiles are flat in the center, the oxidation was not really uniform throughout the bulk, even at the lowest temperature of these tests (600 °C). Since the rate of oxygen supply was about 650 higher than the rate of carbon loss (Fig. 2), there is little reason to assume that oxidation was starved by insufficient supply of oxygen at this temperature. Yet, after 48 h (at 19% weight loss) the density of the core did not change from its initial value; only after 70 h (at 40% weight loss) oxidation reached the center of the 25.5 mm specimens, although more corrosion occurred in the surface layer. At higher temperatures the preferential oxidation of the surface is even more evident. The trend is also evident with the increase of the weight loss. The overall size of oxidized samples did not vary significantly in the initial stages of oxidation (low temperatures, low weight losses); this indicates more or less uniform oxidation in the bulk. In contrast, at higher temperatures and for advanced oxidation levels (77% weight loss in 8 h at 700 °C) corrosion is limited to the surface layer; in these cases the shrinking core scenario seems a more appropriate description.

To describe the development of the preferentially oxidized surface layer, Wichner and Ball introduced the concept of chemically reactive oxidation zone [19]. Combining information from various sources (not necessarily at identical conditions), these authors proposed a quadratic equation to correlate the thickness of active oxidation zone (Δh) with the oxidation temperature. Their data are plotted in Fig. 4, together with the data obtained in the present investigation (Δh was taken as the thickness of surface layer where the density was different from that of the unoxidized core). The best fit was obtained with a quadratic equation, as originally proposed by Wichner and Ball [19]. Although the results do not coincide, they indicate a similar trend. In this instance, however, the quadratic function is just a practical choice to better fit the data. More significant is the proportionality of the corroded zone thickness with the square root of oxidation time (for comparable levels of weight loss), as shown in Fig. 4(b). This indicates the role of diffusion in the radial growth of the oxidized layer. Indeed, it was suggested [31] that the complex nature of the pore system in graphite may enable a dual mechanism of the oxidation process. This is particularly true at the temperatures where the oxidation mechanism shifts from regime 1 to regime 2. While oxidation in macropores (>0.050 μm) and larger voids may continue in the chemical control (gradient-free) regime, oxidation in micropores (<0.002 μm) and mesopores (0.002–0.050 μm) may become diffusion-controlled. In order to understand this effect, more data must be systematically collected in better controlled conditions. This is necessary for the development of predictive computational models for the behavior of large graphite blocks based on data collected on small specimens.

4.3. Slope and intercepts of Arrhenius plots

The activation energy measured in this study for most graphite materials was in the range of 190–210 kJ/mol; an exception was the fuel matrix material for which the activation energy was 160 kJ/mol. Values in the same range were reported previously for oxidation of high purity graphite materials in the chemical control regime (Table 1). In addition, the Arrhenius plots of this study were linear (with one exception); based on previous reports, this might be considered an indication that the oxidation mechanism did not change in the temperature range investigated.

However, analysis of density profiles after oxidation made it obvious that oxidation occurred in fact through a combination of chemical control (regime 1) and in-pore diffusion control (regime 2), even in the temperature range where Arrhenius plots were linear (600–750 °C). The complex structure of graphite causes a continuous transition between the two regimes of oxidation. This leads to the question: is it possible to differentiate oxidation regimes based on the value of activation energy only?

It was suggested that the apparent activation energy for oxidation in regime 2 (in-pore diffusion control) is roughly half of that of the true chemical kinetics control [12]. According to Lewis [33] apparent activation energy lower than about 250 kJ/mol indicates that the experiment was not completely in regime 1, or that catalytic effects marred the experiments. In fact, as Table 1 shows, there are only a few examples of graphite oxidation reports in the literature where activation energies higher than 200–210 kJ/mol

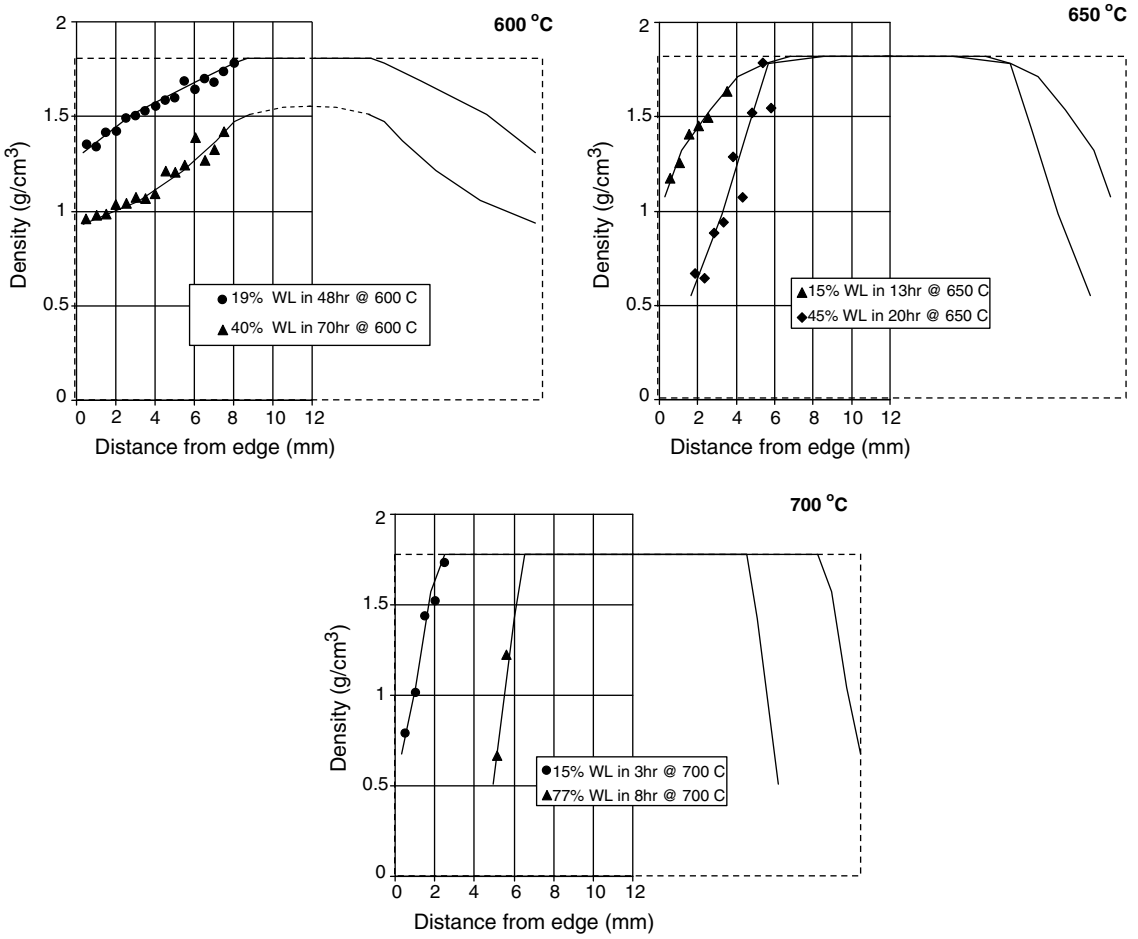

Fig. 3. Density profiles of small grained graphite specimens (R4-650) oxidized in the vertical furnace at different temperatures and two levels of weight loss. Before oxidation all specimens were cylindrical with $D = H = 2.54$ cm. The air flow rate in all tests was 10 L/min. The duration of the oxidation and the final weight loss are indicated for each sample.

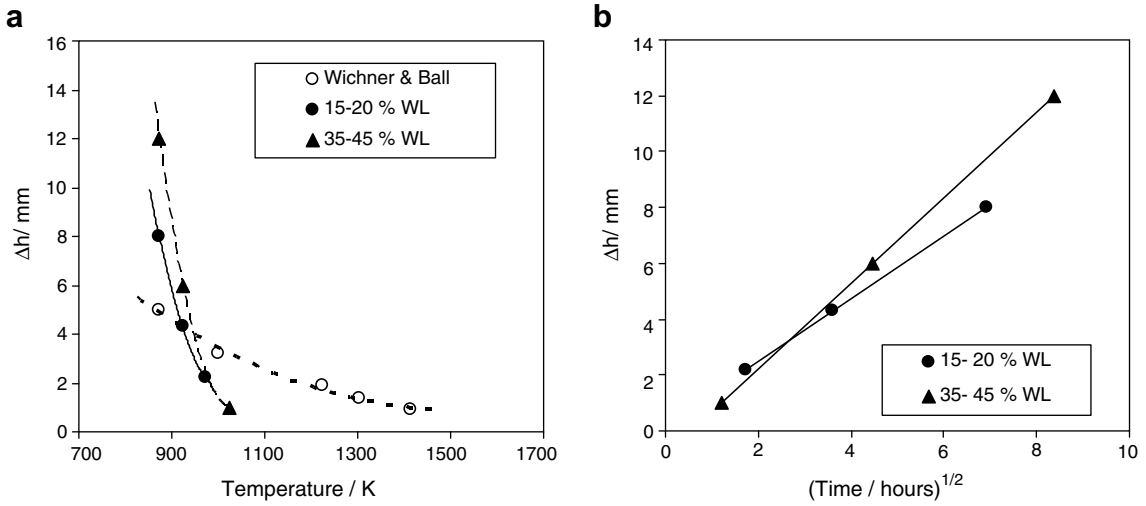

Fig. 4. Empirical correlations showing the dependence of oxidation depth on (a) temperature and (b) time. In (a) the measured oxidation depth was fitted with a quadratic function as suggested by Wichner and Ball [19]. Correlation coefficients are 1.00 for the results of this study (at two different levels of weight loss, WL) and 0.988 for Wichner and Ball data (unknown weight loss). In (b) the linear dependence of the thickness of the oxidized layer with the square root of time (correlation coefficients 1.00 in both examples) suggests a random steps diffusion mechanism.

were measured. Li and Brown [34] demonstrated that the activation energy depends in fact on which is the main oxidation product: if the oxidation product is CO_2 the activation energy could be as large as 270 kJ/mol; however, if CO is the main oxidation product, the activation energy is only 203 kJ/mol. At low temperature the main oxidation product is CO_2, and the equilibrium is

Table 1
Activation energy values reported by previous authors for graphite oxidation in chemical control regime

Material	Activation energy, kJ/mol	Reference
PGX gas purified (500–750 °C)	198	This study
NBG 10 (500–750 °C)	193	This study
R4-650 (500–750 °C)	202	This study
AG 13-01 (600–750 °C)	225	This study
Fuel matrix (500–650 °C)	160	This study
Natural graphite	188	[26]
Synthetic graphite	170	[26]
Spectroscopically pure graphite	200	[32]
Very pure graphite (5 ppm impurity)	250	[33]
Low purity graphite (150 ppm)	168–189	[33]
Nuclear grade graphite IG 110	218	[9]
Nuclear grade graphite IG 110	188	[3]
Nuclear grade graphite IG 11 (400–600 °C)	158	[29]
Nuclear grade graphite IG 11 (600–800 °C)	72	[29]
HTR fuel element – filler	166	[1]
HTR fuel element – binder	123	[1]

shifted towards more CO as the temperature increases. At intermediate temperatures both CO and CO_2 may be formed, which explains why many authors reported apparent activation energies lower than 200 kJ/mol. A high proportion of CO may also result from insufficient air supply at the test conditions. Therefore, there are two factors, temperature and oxygen partial pressure, that contribute to the gradual shift of the reaction from regime 1 to regime 2. This may, or may not, be accompanied by a distinct bending of Arrhenius plots. In fact, the linearity of Arrhenius plots does not necessarily prove that oxidation was in the chemical control regime, and that it was not affected by in pore diffusion.

Apart from comparing the slope of Arrhenius plots (activation energy values), comparing the intercepts is equally important for quantification of the oxidation resistance of various graphite materials. In principle, it should be possible to detect similar trends if a material is characterized on various instruments and using samples of various sizes and shapes, as long as there is sufficient supply of air. In practice, the local conditions during oxidation play a strong role, which determines large differences between the rates of oxidation measured on different instruments. As an example, Fig. 5 shows Arrhenius plots measured for the same material (AG 13-01) on the vertical furnace (VF) using large size specimens ($H = D = 25.4$ mm) and on the commercial TGA using small-size specimens ($H = D = 6$ mm). Although the activation energy values measured in the VF were sensitive to the air flow rate, the average (207 kJ/mol) matches very well the values measured in the TGA (205 kJ/mol). However, when surface-normalized rates (r_a) were used, Eq. (3), the oxidation rates measured in the TGA were about one order of magnitude lower than those measured in the VF (Fig. 5(a)). This is caused by the difference in surface-to-volume ratio between the samples used in the two instruments. When mass-normalized rates (r_m) were used, Eq. (4), the data points from the two setups clustered within a much narrow band (Fig. 5(b)). The difference is not caused by insufficient air supply in the TGA; it is rather caused by the additional term in Eq. (3) which is sensitive to size and shape of the specimens. Although a similar analysis should be extended to more materials and experimental conditions, it is apparent at this point that the size and shape differences between samples can be significantly reduced by using mass-normalized rates, which would provide grounds for comparison of results between various instruments and setups.

4.4. Preferential binder oxidation

One more factor complicating the picture resides in the multiphase composition of graphite. The filler, a calcined petroleum or pitch coke, is less reactive than the binder, a coal tar pitch, which is more disordered and more chemically reactive. The impregnant, if any, is the most chemically reactive component. Metal impurities in any of these phases may have a strong catalytic effect and accelerate the oxidation.

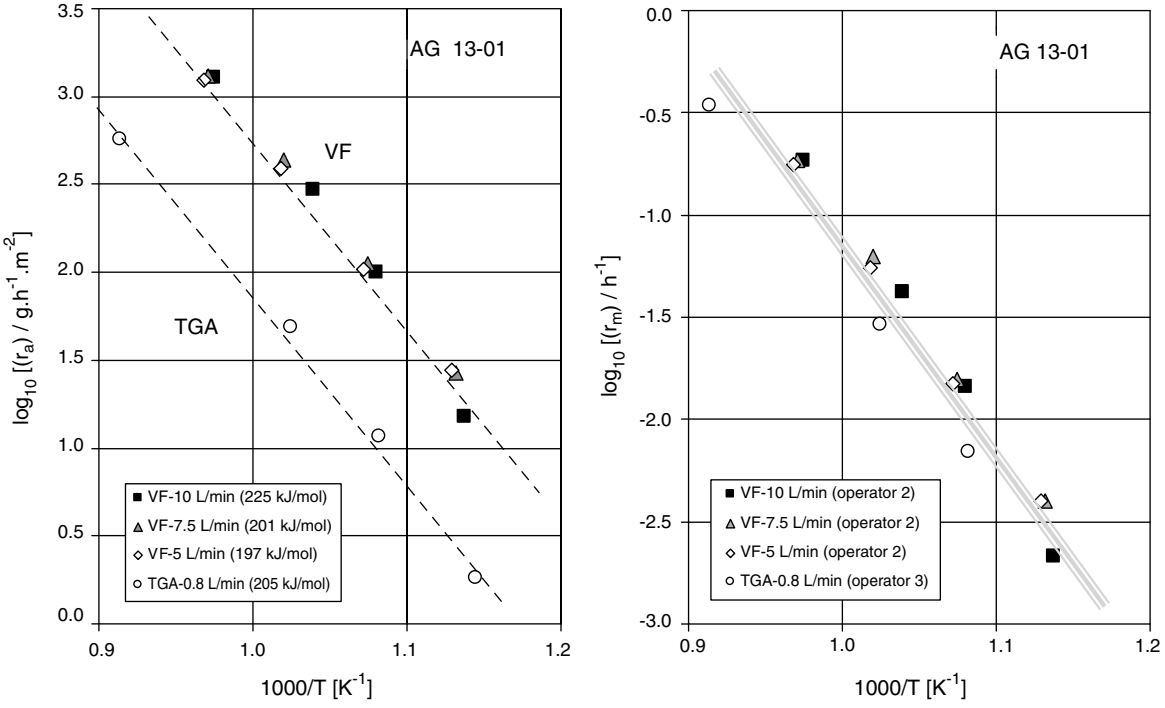

Fig. 5. Arrhenius plots for oxidation of AG 13-01graphite in the vertical furnace (VF) and TGA systems. The oxidation rates were calculated for the 5–10 % burn-off range: (a) in units of g h^{-1} m^{-2} using Eq. (3); and (b) in units of g h^{-1} g^{-1} (or h^{-1}) using Eq. (4). Normalizing oxidation rates to the sample weight minimizes the differences between the TGA and VF results and has no effect on the activation energy.

It was previously reported that degradation of mechanical properties of graphite is connected with preferential oxidation of the binder, propagation of cracks at the binder-filler interface, or development of porosity in the binder [35,36]. In many studies on machined samples the oxidation density gradients within the oxidized samples could not be totally avoided. For example, based on the variation of oxidation rates with the degree of weight loss, Moormann [12] identified the activation energy for oxidation of the binder (123 kJ/mol) and the filler (166 kJ/mol) of HTR fuel element matrix graphite. Although the fast oxidizing binder phase produced a large increase in the rate of weight loss during the course of oxidation up to 750 °C, the process was still considered in the chemical regime [12].

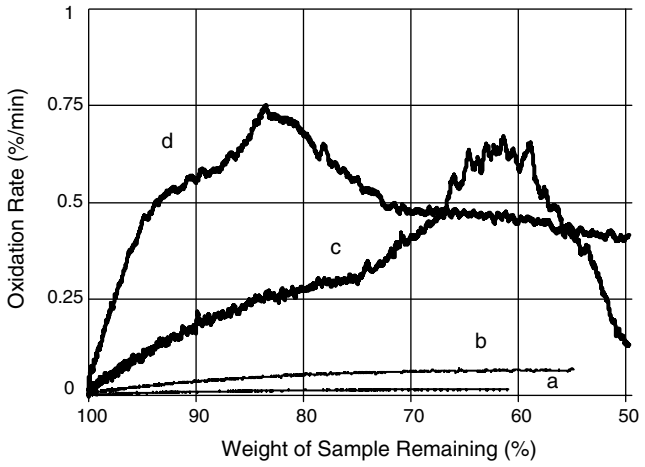

Fig. 6. Variation of the oxidation rate during oxidation of a fine grained graphite (R4-650) at different temperatures: (a) 600 °C for 70 h; (b) 650 °C for 20 h; (c) 700 °C for 8 h; and (d) 750 °C for 4 h. The peaks in the oxidation rate seen at high temperature are caused by preferential oxidation of the most reactive phase (the binder).

Rate variations similar to those reported by Moormann [12] were also identified in the present study. The example in Fig. 6 shows the variation of oxidation rates versus weight loss between 600 and 750 °C during oxidation of the fine grained R4-650 nuclear grade graphite At low temperatures (600–650 °C) the acceleration of oxidation rate is slow, and a practically constant rate is achieved at about 20–30% weight loss. At higher temperatures (700–750 °C) a distinct peak in oxidation rate is apparent in the course of oxidation; as the temperature increases this peak appears earlier in the weight loss process. Such a peak in the isothermal oxidation rate signals preferential oxidation of the most reactive phase as the temperature increases.

4.5. Electron microscopy

The preferential oxidation of the binder phase was analyzed comparatively using scanning electron microscopy (SEM) for coarse grained graphite (AG 13-01) and fine grained graphite (2020). Fig. 7(a) shows the surface of an unoxidized AG 13-01 sample after 5% weight loss at 650 °C, and 90% weight loss at 800 °C. Fig. 7(b) shows the surface of graphite 2020 before oxidation, after 10% weight loss at 600 °C, and after 95% weight loss at 850 °C. The images show the structural changes at the surface of thermally oxidized samples. A gradual development of pits or pores, followed by preferential corrosion of the binder phase, is apparent for both coarse and fine grained graphite. However, the extent of selective oxidation at the surface of the coarse grained graphite appears to be much higher. These results support similar conclusions reported by other authors [37].

4.6. Raman spectroscopy

Raman spectroscopy was used for a closer examination, and possible identification, of the reactive phase that undergoes preferential oxidation. Raman spectra of transversally sectioned graphite specimens were collected using a DilorXY 800 Raman microprobe

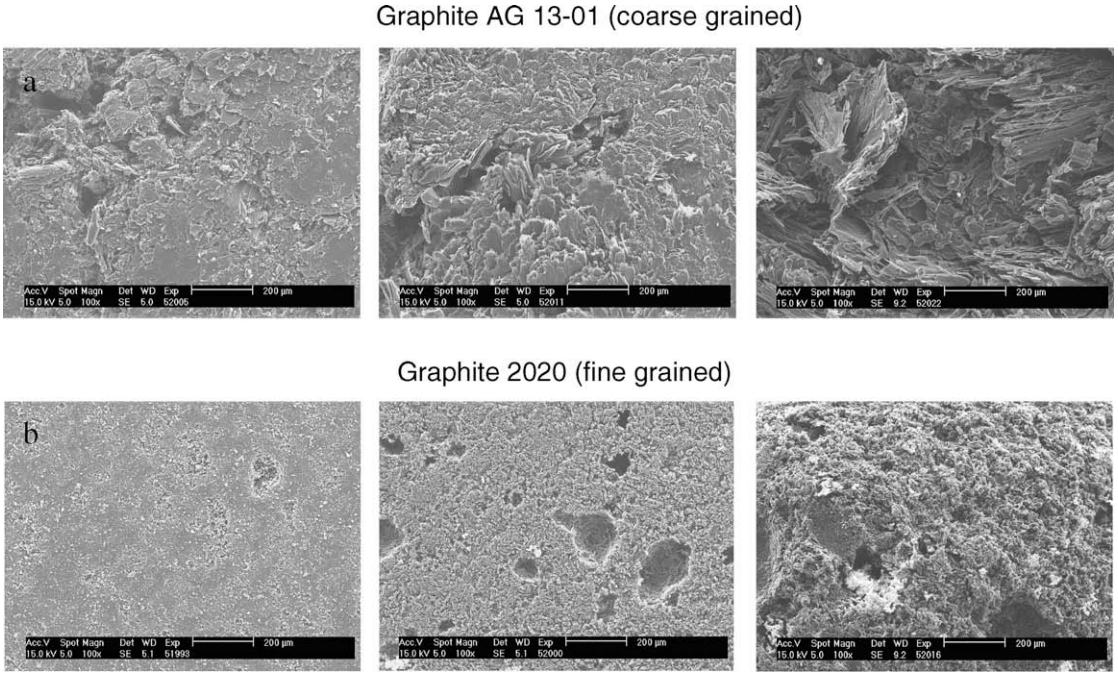

Fig. 7. Scanning electron microscopy images of the surface of graphite samples of different grain sizes at various levels of oxidation showing preferential binder oxidation. Upper row: coarse grained graphite (AG 13-01) before oxidation and after oxidation at 5% and 90% weight loss. Lower row: fine grained graphite (2020) before oxidation and after oxidation at 10% and 95% weight loss. The size bar of every micrograph is 200 μm.

(JY, Inc., Edison, NJ) with an Innova 308c Ar^+ laser (Coherent, Inc., Santa Clara, CA) operating at 5145 Å and 500 mW output power. In order to accommodate the microstructure of the material (PGX graphite) which showed features of 10 μm in size or larger, the 10× objective lens was used and defocused to a spot size of ~100 μm so as to better collect an average spectrum from the sample, and to minimize laser heating. Fifty spectra were collected from both the center and within 1 mm of the edge of two samples oxidized (up to 15% weight loss) to 700 and 750 °C; they were compared with spectra collected at similar positions of the unoxidized material. Fig. 8 shows the averaged Raman spectra recorded for the three samples. The D (disorder) and G (graphite) Raman bands at ~1350 cm^{-1} and ~1580 cm^{-1} respectively were fitted with a pseudo-Voigtian function and a linear baseline from which the G/D intensity ratios were calculated.

Laser Raman spectra recorded at the center (dotted line) and at 1 mm from the edge (solid line) of transversally sectioned graphite specimens (PGX gas purified): (a) before oxidation; and after oxidation (to 15% weight loss) at (b) 700 °C and (c) 750 °C.

Table 2 shows the G/D Raman intensity ratios at both regions (center and 1 mm from edge) of all three samples. A distinct trend can be seen, namely the G/D ratios of both oxidized samples are larger than those of the unoxidized material; however, the absolute G/D values decline slightly between samples oxidized at 700 °C and 750 °C. For all three samples, the G/D ratio is higher in the center than at the edge.

Interpreting the Raman spectra of carbonaceous materials can be difficult since it is dependent on factors such as the excitation frequency and laser power, the crystallite size and stoichiometry, and the type of bonding; oxidation only complicates the matter. Nevertheless, some basic conclusions can be reached if one recognizes two general trends in the Raman spectra of carbon forms, namely higher G/D intensity ratios indicate a better ordered component (i.e. filler) and smaller crystallite sizes [38]. The material analyzed here is initially quite complex since it has two-phases of different form, filler and binder. It is reasonably to associate the G (graphitic) band with the better ordered domains in the filler and the D (disordered) band with the weaker and more disordered binder phase.

Table 2
Ratio of G/D band intensities of Raman spectra from Fig. 8

Sample	Center G/D	Standard deviation	Edge G/D	Standard deviation	G/D center/edge
Unoxidized	2.48	0.60	2.27	0.52	1.09
700 °C	4.45	0.67	3.99	0.63	1.11
750 °C	4.00	1.18	3.08	0.25	1.30

The last column in Table 2 compares the G/D ratios between the center and the edge of each sample. The numbers clearly increase with the increase in oxidation temperature. Following the above rationale it appears that the edge of oxidized samples contains a larger proportion of the more ordered phase. This is a direct confirmation that the phase which is preferentially oxidized at the edge of the samples is the more disordered phase (with a smaller G/D ratio), i.e. the binder.

4.7. Significance of results

From the above discussion it is apparent that separating diffusion effects from kinetically controlled oxidation of graphite is problematic, especially when using large specimens that can be considered as representative for a given material. It was suggested that comparative studies on graphite powders and on machined specimens can possibly sort out the contribution of in-pore limited diffusion for large samples [35]. Even so, preferential oxidation of the binder which causes non-uniform density distributions in the oxidized sample is difficult to avoid. Oxidation gradients can be avoided while still using large samples (in the range of centimeters) by selecting lower oxidation temperature (in the range of 400–500 °C) but this can hardly be accommodated with the objective of maximizing the number of tests that can be done in a given period of time. Another option is comparing oxidation rates at lower levels of weight loss, which would allow shortening the duration

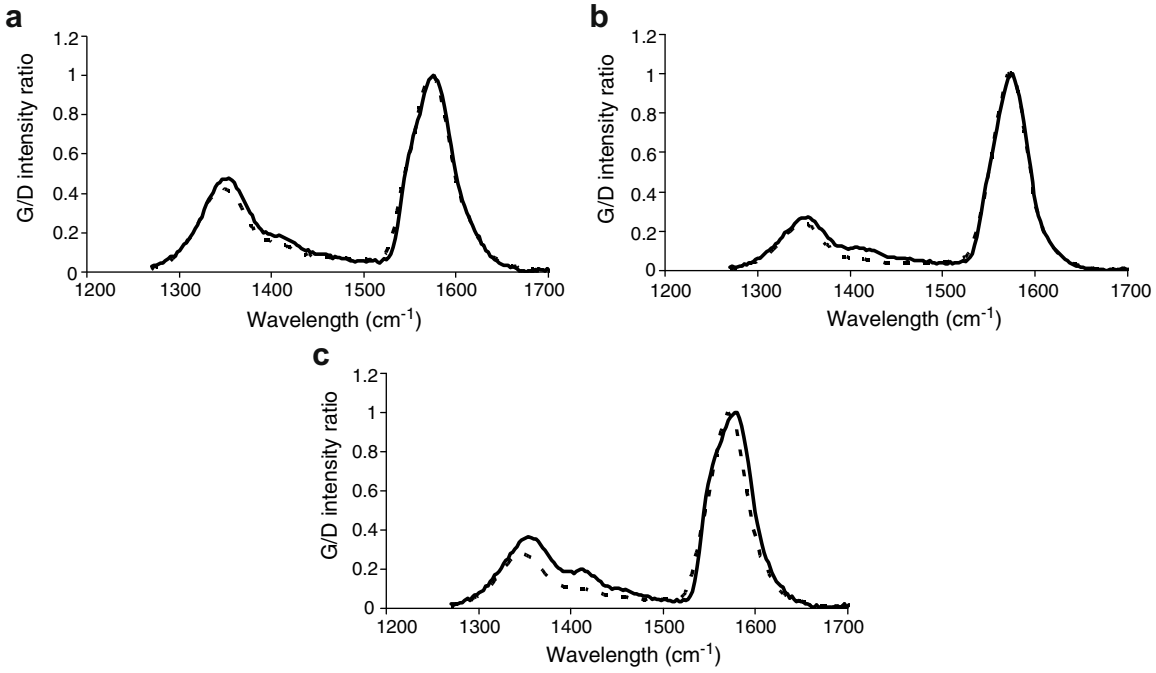

Fig. 8. Laser Raman spectra recorded at the center (dotted line) and at 1 mm from the edge (solid line) of transversally sectioned graphite specimens (PGX gas purified): (a) before oxidation; and after oxidation (to 15 % weight loss) at (b) 700 °C and (c) 750 °C.

of tests. It was reported [3,18] that the activation energy remains constant in the course of oxidation, and that the factor that determines the variation of the oxidation rate with the burn-off is the gradual development of the internal surface through the porous graphite body. The rates reported in this study were calculated between 5 and 10% weight loss, while other authors chose to report only initial oxidation rates [4,9,18]. The reliability of rate measurements in the so-called 'induction period' of early oxidation stages needs to be confirmed in an inter-laboratory test.

On the other hand, the merit of standardizing the test conditions with respect to sample size and shape, air flow rate, and the geometry of the oxidation tube should be recognized. A question still remains however about the significance of the test results obtained in the transition zone between oxidation regimes 1 and 2. In other words, an acceptable limit for diffusion-induced perturbations on the accuracy of test results and the significance of comparison of oxidation rates for samples with non-uniform oxidation profiles still must be determined.

In principle, graphite oxidation can be modeled based on intrinsic kinetic rate parameters (obtained from measurements on powders and free of diffusion perturbations) using finite elements analysis to describe gas diffusion and corrosive reactions at pore walls in complex porous bodies, and computational fluid dynamics for the gas phase. Although some notable progress has recently been made [39] this exercise is still difficult because of the complexity of computation tasks. Predictive models are needed for a more accurate description of materials behavior under different scenarios, including an air ingress incident. The MELCOR code was originally developed by Sandia National Laboratory for analysis of severe core damage accidents in nuclear reactor systems [40]. This is a thermal-hydraulic reactor accident code which was subsequently modified to include graphite oxidation parameters [41], and was used for modeling an air ingress accident in a PBMR reactor [42].

To put the results reported here in a broader perspective, the input data on graphite oxidation rates employed in the MELCOR analysis of air ingress accidents [43] are compared in Fig. 9 with the oxidation rates measured in this study in standardized conditions. In this figure, the oxidation rates used for the MELCOR analysis cover a broad range; they were estimated from two series of measurements at Idaho National Engineering and Environmental Laboratory using materials with very different oxidation resistance: a low reactivity carbon fiber composite impregnated with pyrolitic carbon (INEEL 2002) [44], and a more reactive porous graphite (INEEL 1988) [45]. As Fig. 9 shows, the differences between materials are significant in the low temperature range (regime 1) and gradually diminish at high temperatures (regimes 2 and 3), where bulk oxidation transforms into a surface corrosion process. Overlapped over the original data plot from Ref. [43] are the results measured in this study (Fig. 2) normalized in comparable units. The results of this study are within the limits known previously from other studies. Subtle differences can however be observed: in the temperature range of chemical regime, the rates of nuclear grade graphites measured in this study are about one order of magnitude larger than the lowest rates (INEEL 2002) [44] used for model predictions by MELCOR. It appears also that the fuel matrix compacts (incompletely graphitized) have large oxidation rates, very close to the material with low oxidation resistance reported previously (INEEL 1998) [45].

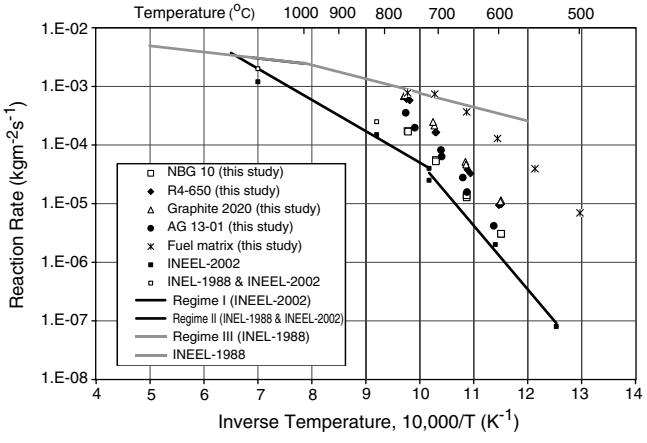

Fig. 9. Comparison of graphite oxidation rates measured in this study with previously reported data (INEEL 1988 and INEEL 2002). The linear trends represent experimental results for materials of different oxidation resistance. Oxidation rates derived for the material with the lowest reactivity (INEEL 2002) served as input information for analysis of air ingress accidents using the modified MELCOR code. Figure adapted from Ref. [43].

It can be concluded that, in spite of limitations caused by non-uniform oxidation profiles of large graphite specimens, standardizing the test method for measuring oxidation rates offers reliable results. The completion of the inter-laboratory study for the proposed standard test method, currently in progress, will show the repeatability and the bias limits of the method. Such measurements have practical significance, and are needed for a better understanding of the effect of temperature on thermal oxidation of various grades of graphite in air. A test method based on standardized specimen sizes and shapes, air flow rates, and geometry of the testing tube has its value as a tool for the designer, interested in selection of best performing materials. It will also help increase the reliability and accuracy of predictive models based on graphite oxidation rates and increase the degree of safety of nuclear systems even in the worst case scenarios. However, more research effort is required for development and validation of predictive computational models applicable to oxidation of large blocks of graphite in conditions where process is controlled by the interplay between kinetic and diffusion effects.

Acknowledgments

This research was funded by the US Department of Energy, Office of Nuclear Energy Science and Technology under contract DE-AC05-00OR22725 with UT Battelle, LLC. The authors acknowledge the fruitful exchange of ideas with Drs Gary Pruett (Goodrich Corp., USA), Anthony Wickham (University of Manchester, UK), Martin Metcalfe (NexiaSolutions, UK), Se-Hwan Chi (KAERI, Korea), and Shri Awasthi (HITCO Carbon Composites, Inc.). Invaluable discussions with Dr. Bob Wichner (ORNL) and contributions of colleagues Joseph Kelly, Ashli Clark, and ORAU-ORISE intern students Chinwe Onuorah (HERE program) and Zack Vance (SULI program) are greatly appreciated.

References

[1] R. Moormann, H.-K. Hinssen, K. Kuhn, Nucl. Eng. Design 227 (2004) 281.
[2] C.I. Contescu, F.S. Baker, T.S. Burchell, in: Extended Abstracts of CARBON '06, International Carbon Conference, Aberdeen, Scotland, 16–24 July 2006.
[3] E.L. Fuller, J.M. Okoh, J. Nucl. Mater. 240 (1997) 241.
[4] W. Jiang, G. Nadeau, K. Zaghib, K. Kinoshita, Thermochim. Acta 351 (2000) 85.
[5] A.K. Bhattacharya, P. Bandopadhyay, P. Das, Ceram. Int. 29 (2003) 967.
[6] J.R. Hahn, Carbon 43 (2005) 1506.
[7] O.C. Kopp, E.L. Fuller, A.D. Surrett, J. Nucl. Mater. (1993) 333.
[8] K.Y. Cho, K.J. Kim, D.H. Rui, S.W. Chi, J.K. Hong, in: Extended Abstracts of CARBON '06, International Carbon Conference, Aberdeen, Scotland, 16–24 July 2006.
[9] E.S. Kim, W.W. Lee, H.C. No, J. Nucl. Mater. 348 (2006) 174.
[10] T.J. Clark, R.E. Woodley, D.R. deHalas, Gas-Graphite Systems, in: R.E. Nightingale (Ed.), Nuclear Graphite, Academic Press, New York, 1962, p. 387.
[11] W.A. Propp, Graphite Oxidation: Thermodynamics/Reactions, DOE/SNF/REP-018, September, Idaho National Engineering and Environmental Laboratory, 1988.

[12] R. Moormann, H.K. Hinssen, A. K Krussenberg, B. Stauch, C.H. Wu, J. Nucl. Mater. 212–215 (1994) 1178.
[13] ASTM D 7219-05, Standard specification for isotropic and near-isotropic nuclear graphite (approved November 1, 2005; published December 2005).
[14] ASTM C 709-03a, Standard terminology relating to manufactured carbon and graphite (approved November 1, 2003; published November 2003).
[15] M.B. Richards, Energy 15 (1990) 729.
[16] ASTM subcommittee D02-F, draft of "Standard test method for determination of fracture toughness of graphite at ambient temperature", work item number 9689, 11 April 2006.
[17] ASTM subcommittee D02-F, draft of "Standard practice for reporting uniaxial strength data and estimating Weibull distribution parameters for polycrystalline graphite", Designation C Rev. 1-06, 25 June 2006.
[18] E.S. Kim, H.C. No, J. Nucl. Mater. 349 (2006) 182.
[19] R.P. Wichner, S.J. Ball, Potential Damage to Gas-Cooled Graphite Reactors Due to Severe Accidents ORNL/TM-13661, Oak Ridge National Laboratory, Oak Ridge, TN, 1999.
[20] Moore, R. L., C. H. Oh, B. J. Merrill, D. A. Petti, in: Proceedings of HTR 2002, First International Topical Meeting on High Temperature Reactor Technology (HTR), Petten, Netherlands, 22–24 April 2002.
[21] R.H. Hurt, B.S. Haynes, On the origin of power law kinetics in carbon oxidation, in: Proc. Combustion Institute 30 (2005) 2161–2168.
[22] G. Blyholder, H. Eyring, J. Phys. Chem. 61 (1957) 682.
[23] R.T.K. Baker, P.S. Harris, Carbon 11 (1973) 25.
[24] E.A. Gulbransen, K.F. Andrew, Ind. Eng. Chem. 44 (1952) 1034.
[25] A.-K. Krussenberg, R. Moormann, H.-K. Hinssen, M. Hofmann, C.H. Wu, J. Nucl. Mater. 258–263 (1998) 770.
[26] K. Zaghib, X. Song, K. Kinoshita, Thermochim. Acta 371 (2001) 57.
[27] General Atomics, Graphite Design Handbook, DOE-HTGR-88111, 1988.
[28] C. Velasquez, G. Hightower, R. Burnette, The oxidation of H-451 graphite by steam, GA-A14951, UC-77, 1978.
[29] L. Xiaowei, R. Jean-Charles, Y. Suyuan, Nucl. Eng. Design 227 (2004) 273.
[30] P. Hawtin, J.A. Gibson, R. Murdoch, J.B. Lewis, Carbon 2 (1964) 299.
[31] M. Eto, F.B. Growcock, Carbon 21 (1983) 135.
[32] L.R. Radovic, P.L. Walker Jr., R.G. Jenkins, Fuel 62 (1983) 849.
[33] J.B. Lewis, in: L.C.F. Blackmun (Ed.), Modern Aspects of Graphite Technology, Academic Press, 1970, p. 39.
[34] C. Li, T.C. Brown, Carbon 39 (2001) 232.
[35] J.L. Wood, R.C. Bradt, P.L. Walker Jr., Carbon 18 (1980) 179.
[36] T.D. Burchell, I.M. Pickup, B. McEnaney, R.G. Cooke, Carbon 24 (1986) 545.
[37] I.M. Pickup, B. McEnaney, R.G. Cooke, Carbon 24 (1986) 535.
[38] S. Reich, C. Thomsen, Phil Trans. R. Soc. Lond. A 362 (2004) 2271.
[39] E.S. Kim, H.C. No, J. Nucl. Mater. 349 (2006) 182.
[40] <http://www.ofcm.gov/atd_dir/pdf/melcor.pdf> (accessed 10.14.06)
[41] B.J. Merrill, R.L. Moore, S.T. Polkinghorne, D.A. Petti, Fusion Eng. Design 51–52 (2000) 555.
[42] R. L. Moore, C. H. Oh, B.J. Merrill, D.A. Petti, in: *Proc. Conf. High Temperature Reactors, Petten, NL, 22–24 April 2002, Publ. HTR-2002, p. 1–5*, International Atomic Energy Agency, Vienna; <http://www.iaea.org/inis/aws/htgr/fulltext/htr2002_701.pdf> (accessed 10.14.04).
[43] D.A. Petti, T.J. Dolan, G.K. Miller, R.L. Moore, W.K. Terry, A.M. Ougouag, C.H. Oh, H.D. Gougar, Modular Pebble-Bed Reactor Project, INEEL/EXT-02-01545, 2002.
[44] M.H. O'Brien, B.J. Merrill, S.N. Ugaki, Combustion Testing and Thermal Modeling of Proposed CIT Graphite Tile Material, EGG-FSP-8255, September, Idaho National Engineering Laboratory, 1988.
[45] T.D. Marshall et al., Air Chemical Reactivity Measurements of the Carbon Fiber Composite NB31, INEEL/EXT-02-00745, Idaho National Engineering and Environmental Laboratory, 2002.